tics of the singlet-singlet $\pi-\pi^*$ transition and reproduce the exciton CD pattern, for the following reasons. First, the CD behaviors are consistent with the theoretically anticipated pattern; that is, two CD bands in the charge-transfer region reproduce the exciton CD splitting in the long-axis-polarized $\pi-\pi^*$ transition region. Second, the CD spectrum of $(+)_{546}[Cr(acac)(acaBr)(en)]^+$ is similar to those of $(+)_{546}$-$[Cr(acac)_2(en)]^+$ and $(+)_{546}[Cr(acaBr)_2(en)]^+$ in both the charge-transfer and the $\pi-\pi^*$ transition regions. Third, two CD pairs of $(+)_{546}[Cr(acac)(acaBr)(en)]^+$ are found to be at the intermediate position between $(+)_{546}[Cr(acac)_2(en)]^+$ and $(+)_{546}[Cr(acaBr)_2(en)]^+$ as may be predicted by the exciton model[4] (Table II and Figures 6 and 7). Fourth, if the CD bands (+) at 30.5 kK and (−) at 34.5 kK originate from the charge-transfer transition, the mono- and bis-acetylacetonato complexes may show similar CD patterns in this region. This is not the finding.

The remaining two CD bands at the lowest and the highest frequency for $(+)_{546}[Cr(acac)_2(en)]^+$, (−) at 29.1 kK and (−) at 44.7 kK, may be ascribed to $V_2(E)$ and $V_8(E)$, respectively, from the lower frequency side.

The assignment for the ultraviolet CD bands of the 3-halogenoacetylacetonato complexes may be made similarly to those of the bis-acetylacetonato complex as is seen in Table II.

On the basis of the signs of two CD pairs due to the exciton splitting, the absolute configuration of $(+)_{546}[Cr(acac)_2(en)]^+$ and its 3-halogeno derivatives is determined to be Λ in accordance with the dominance of positive CD in the first ligand field band region. This assignment is also consistent with that of $\Lambda-(+)_{589}[Cr((+)atc)_3]$, which shows visible and ultraviolet CD spectra[26] similar to those of $(+)_{546}[Cr(acac)_2(en)]^+$ and its 3-halogeno derivatives and whose absolute configuration has been determined by means of an X-ray method.[27]

Registry No. [(dip)(phen)Cr(OH)_2Cr(dip)(phen)](NO_3)_4·6H_2O, 36537-23-2; (−)-[Cr_2(OH)_2(dip)_2(phen)_2](NO_3)_4·7H_2O, 36537-24-3; [Cr(OH)(OH_2)(dip)(phen)](NO_3)_2·1.5H_2O, 36487-19-1; (−)-[Cr_2(OH)_2(dip)_4]Cl_4·9H_2O, 36544-33-9; (−)-[Cr_2(OH)_2(phen)_4](NO_3)_4·7H_2O, 36544-34-0; [Cr(ox)(dip)(phen)]Cl, 36544-35-1; (−)-[Cr(ox)(dip)(phen)]·ClO_4·2H_2O, 36538-29-1; (−)-[Cr(ox)(dip)(phen)][Cr(ox)_2(phen)]·3H_2O, 12769-30-1; (−)-[Cr(ox)(dip)_2]Cl·4H_2O, 23539-88-0; (−)-[Cr(ox)(phen)_2]ClO_4·2.5H_2O, 36544-37-3; [Cr(acac)(en)_2]Cl_2·5H_2O, 36544-31-7; [Cr(acac)(en)_2]I_2, 36544-32-8; (+)-[Cr(acac)(en)_2]Cl_2·H_2O, 36544-02-2; (+)-[Cr(acac)(en)_2][As_2(L-tart)_2]·3H_2O, 12769-26-5; (+)-[Cr(acaBr)(en)_2]Cl_2·2.5H_2O, 36544-03-3; (+)-[Cr(acac)-(en)_2]Cl_2·H_2O, 36544-02-2; (+)-[Cr(acaCl)(en)_2]Cl_2·1.5H_2O, 36544-05-5; [Cr(acac)_2(en)]Cl·1.5H_2O, 36544-06-6; [Cr(acac)_2(en)]I·H_2O, 36544-07-7; (+)-[Cr(acac)_2(en)]Cl·6.5H_2O, 36544-08-8; [Cr(acaBr)_2(en)]Cl·2H_2O, 36544-09-9; (+)-[Cr(acaBr)_2(en)]_2ClBr, 12769-27-6; (+)-[Cr(acaCl)_2-(en)]Cl·H_2O, 36544-10-2; [Cr(acac)(acaBr)(en)]Cl·2H_2O, 36544-11-3; (+)-[Cr(acac)(acaBr)(en)]Cl·H_2O, 36544-12-4.

(27) W. D. Horrocks, Jr., D. L. Johnston, and D. MacInnes, *J. Amer. Chem. Soc.*, **92**, 7620 (1970).

Contribution from the Department of Chemistry, Faculty of Science, Osaka University, Toyonaka, Osaka, Japan

Circular Dichroism of Chromium(III) Complexes. IV.[1] Elucidation of Circular Dichroism in the Spin-Forbidden Transitions

SUMIO KAIZAKI, JINSAI HIDAKA,* and YOICHI SHIMURA

Circular dichroism (CD) spectra of 19 optically active chromium(III) complexes have been measured in the spin-forbidden and the spin-allowed d–d transition region. It has been revealed that the rotational strengths for the spin-forbidden transitions are theoretically related to those for the spin-allowed transitions. On the basis of this relationship, the CD peaks in the spin-forbidden transition region have been assigned to the zero-field splitting components of the doublet state in connection with the CD bands in the first spin-allowed transition region and also with the absolute configurations of the complexes.

Introduction

The absorption spectra of most chromium(III) complexes show in the visible region two broad but moderately intense bands associated with the d-d Laporte-forbidden but quartet–quartet spin-allowed transitions and in the near-infrared region weak but sharp bands associated with the doublet–quartet spin-forbidden transitions. There have been a number of investigations[2] concerning the latter spin-forbidden transitions for various types of chromium(III) complexes. The spin-forbidden absorption bands are notoriously difficult to observe in solution, because these bands are not only of very low intensity but are also obscured by the strong high-frequency spin-allowed absorp-

tion bands. As to the position of the 0–0 band of the spin-forbidden transitions, the phosphorescence measurement[3,4] is a useful technique, but other higher energy components of the doublet states cannot be detected by means of this method. McCaffery, Stephens, and Schatz[5] reported that the magnetic circular dichroism (MCD) in the spin-forbidden transitions of chromium(III) complexes was much more intense than in the spin-allowed transitions. They stated that MCD can greatly aid in the detection and assignments of the spin-forbidden transitions. However, since the observed MCD curves may consist of the dispersion

(1) Part III: S. Kaizaki, J. Hidaka, and Y. Shimura, *Inorg. Chem.*, **12**, 135 (1973).

(2) L. S. Forster, *Transition Metal Chem.*, **5**, 1 (1969).

(3) G. B. Porter and H. L. Schlafer, *Z. Phys. Chem. (Frankfurt am Main)*, **38**, 227 (1963).

(4) G. B. Porter and H. L. Schlafer, *Z. Phys. Chem. (Frankfurt am Main)*, **40**, 280 (1964).

(5) A. J. McCaffery, P. J. Stephens, and P. N. Schatz, *Inorg. Chem.*, **6**, 1614 (1967).

type curve (*A* term) and the absorption type curve (*C* term), the analyses of these curves require the temperature dependence measurements. On the contrary, natural circular dichroism (CD), which exhibits only the absorption type curve (approximately gaussian) with either a positive or a negative sign, is a more powerful and useful technique for resolving the zero-field splitting components of the overlapping absorption bands. No systematic data on the CD spectra in the spin-forbidden transition region have been accumulated and no detailed theoretical argument has been made until now.

Kling and Woldbye[6] obtained the rotatory dispersion of $(+)_{546}[Cr(en)_3](ClO_4)_3$ and $(+)_{546}[Cr(tn)_3]Cl_3$ in their spin-forbidden absorption band region and found many dispersions superimposed on each other. Mason, *et al.*, reported the CD spectra of tris(L-tartrato)chromium(III) ion[7] and of $(-)_{589}[Cr_2(OH)_2(dip)_4]^{4+}$ or $(-)_{589}[Cr_2(OH)_2 \cdot (phen)_4]^{4+}$ [8] in the spin-forbidden band region. The present authors[9] observed the CD spectra of 12 optically active chromium(III) complexes containing three bidentate ligands in the region concerned and proposed the correlation between the CD bands and the absolute configurations.

In this paper, the CD data of many chromium(III) complexes in solution at room temperature will be reported. The theoretical relationship between the rotational strengths for the spin-forbidden transitions and those for the spin-allowed transitions will be derived from a crystal field treatment. The CD bands in the spin-forbidden transition region will be assigned in detail and will be also correlated with the absolute configurations of the complexes.

Experimental Section

Materials. The preparations and optical resolutions of all the chromium(III) complexes concerned were described in parts II[9] and III[1] of this series.

Measurements. The electronic absorption spectra were measured by a Beckman DU spectrophotometer. The CD spectra were recorded with a Roussel-Jouan Dichrograph. The concentrations of the complexes for the CD measurements in the spin-forbidden band region were $10^{-1}-10^{-2}$ *F*, and the cell lengths employed were 5 and 7 cm.

Results and Discussion

General Considerations. The present complexes contain three bidentate ligands and belong to D_3 or pseudo-D_3 symmetry. The splitting of energy levels of octahedral d^3 complexes in the trigonal field occurs as shown in Figure 1. The first excited quartet state ($^4T_{2g}$) in octahedral symmetry splits into two components, ^4E and $^4A_1$ in trigonal symmetry, while the doublet states break down into three components, *i.e.*, ^2E_g remaining as the ^2E state and $^2A_2$ and ^2E deriving from the octahedral $^2T_{1g}$ state. Among the three doublet components of d-d transitions, the $^2A_2 \leftarrow {}^4A_2$ transition is not only spin forbidden but also orbitally forbidden. According to the double-group treatment, in which the spin state is taken into account, the ^2E and $^2T_1$ states are split into two and three Kramers doublets, respectively, as indicated in a column D_3' of Figure 1. Although the quartet ground state also breaks down into two Kramers doublets in D_3', the splitting interval[2] was found to be too small to be resolved by the room-temperature spectral measurements in solution. Thus, the zero-field splitting
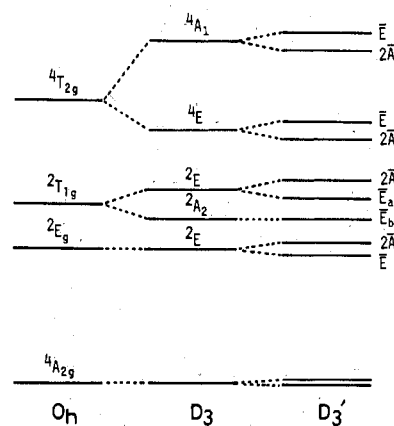
(6) O. Kling and F. Woldbye, *Acta Chem. Scand.*, **15**, 704 (1961).

(7) A. J. McCaffery and S. F. Mason, *Trans. Faraday Soc.*, **59**, 1 (1963).

(8) S. F. Mason, *Inorg. Chim. Acta, Rev.*, **2**, 89 (1968).

(9) S. Kaizaki, J. Hidaka, and Y. Shimura, *Bull. Chem. Soc. Jap.*, **43**, 1100 (1970).

Figure 1. Energy levels for a chromium(III) ion without spin–orbit coupling (O_h, D_3) and with spin–orbit coupling (D_3').

of the ground state is ignored throughout the following discussion. In fact, the detailed physical investigations[10] concerning so-called R lines of ruby, in which chromium-(III) ions are doped as impurities, have revealed that the doublet–quartet electronic transitions $^2E \leftarrow {}^4A_2$ and $^2T_1 \leftarrow {}^4A_2$ consist of five sharp lines.

On the other hand, quantum mechanically, the spin-forbidden transitions may be made allowed by the mixing of the upper quartet states through the perturbation, *i.e.*, the spin–orbit coupling, $\langle\phi(^2\Gamma)|H_{so}|\phi(^4\Gamma')\rangle$.[11] Thus, $\phi(^2\Gamma)$ contains admixtures of $\phi(^4\Gamma')$. The real doublet wave function is given by

$$\Phi(^2\Gamma) = \phi(^2\Gamma) + b\phi(^4\Gamma') \tag{1}$$

where

$$b = \frac{\langle\phi(^2\Gamma)|H_{so}|\phi(^4\Gamma')\rangle}{\Delta E} \tag{2}$$

ΔE represents the energy separation between the doublet state ($^2\Gamma$) and the quartet excited state ($^4\Gamma'$). In other words, the spin-forbidden transitions attain the dipole strength by acquiring a small part, *b*, of the electric dipole moment of the quartet-quartet transitions as given by the equation

$$D(^2\Gamma) = b^2 D(^4\Gamma') \tag{3}$$

For chromium(III) complexes, $^4T_2$ and $^4T_1$ are taken as $^4\Gamma'$. Concerning the rotational strength, it is a good assumption that only the $^4T_2 \leftarrow {}^4A_2$ magnetic dipole allowed transition need be taken into account. In the D_3 single group, the ^2E state may be scrambled only with the $^4E(^4T_2)$ state of the same orbital symmetry. This is the case of Mason's[7] and also the authors'[9] previous treatments. From the detailed polarized crystal spectral studies of ruby[12] and of $NaMg[Cr(ox)_3] \cdot 9H_2O$,[13] it has been revealed that the absorption bands due to the $^2E \leftarrow {}^4A_2$ transitions are observed in both the σ and the π spectra. Therefore, the ^2E state can be mixed with both the $^4A_1$ and ^4E states as expected from the selection rule for the electric dipole transition in the D_3' double group (Table I). However, the group theoretical treatment is limited to the qualitative understanding of the doublet–quartet mixing. In order to

(10) W. Low, *J. Chem. Phys.*, **33**, 1162 (1960); J. Margerie, *C. R. Acad. Sci.*, **255**, 1598 (1962).

(11) E. U. Condon and G. H. Shortley, "The Theory of Atomic Spectra," Cambridge University Press, New York, N. Y., 1935.

(12) S. Sugano and I. Tsujikawa, *J. Phys. Soc. Jap.*, **13**, 899 (1958).

(13) O. S. Mortensen, *J. Chem. Phys.*, **47**, 4215 (1967).

Table I. Selection Rules for the Electric and Magnetic Dipole Transitions in D_3 (Single) and D_3' (Double) Group[a]

D_3	A_1	A_2	E		D_3'	$2\bar{A}$	$\bar{E}$
A_1	X	‖	⊥		$2\bar{A}$	‖	⊥
A_2	‖	X	⊥		$\bar{E}$	⊥	‖, ⊥
E	⊥	⊥	⊥, ‖				

[a] X, forbidden; ⊥ and ‖, allowed with the polarization perpendicular and parallel, respectively, to the trigonal axis (C_3). $\bar{E} = \Gamma_6$; $2\bar{A} = \Gamma_4, \Gamma_5$.

Table II. Rotational Strengths for the $^2\Gamma \leftarrow {}^4A_2$ Transitions[a]

$^2\Gamma$		$R(^2\Gamma)$ ($\zeta'^2/18(\Delta E)^2$ as units)
^2E	$\begin{cases} 2\bar{A} \\ \bar{E} \end{cases}$	$\left.\begin{array}{l} 24R(^4A_1) + 12R(^4E) \\ 8R(^4A_1) + 20R(^4E) \end{array}\right\} 32[R(^4A_1) + R(^4E)]$
$^2T_1$	$\begin{cases} \bar{E}_b \\ 2\bar{A} \\ \bar{E}_a \end{cases}$	$\left.\begin{array}{l} 8R(^4A_1) + 2R(^4E) \\ R(^4A_1) + 7R(^4E) \\ 3R(^4A_1) + 3R(^4E) \end{array}\right\} 12[R(^4A_1) + R(^4E)]$

[a] $\Delta E = E(^2\Gamma) - E(^4T_2)$. The notations for the zero-field splitting components of the doublet states are in accord with Sugano and Tanabe.[14]

obtain the quantitative understanding of the mixing, Sugano and Tanabe[14] have evaluated the theoretical relationship between the dipole strengths for the spin-forbidden transitions on the basis of the crystal field theory with nonzero spin-orbit coupling and with the trigonal field in the absence of vibronic contribution and have successfully applied the resulting relationship to the semiquantitative interpretation for the optical anisotropy and the Zeeman effect of the doublet–quartet transitions in ruby. A similar theoretical treatment will be extended to the rotational strengths for the spin-forbidden transitions of chromium(III) complexes as follows.

Rotational Strengths for the Spin-Forbidden Transitions. The quantum mechanical theory[15] defines the rotational strength, $R(^2\Gamma)$, as the scalar product of the electric and the magnetic dipole moments of the transition $^2\Gamma \leftarrow {}^4A_2$

$$R(^2\Gamma) = \text{Im}\langle^2\Gamma|P|^4A_2\rangle \cdot \langle^4A_2|M|^2\Gamma\rangle \tag{4}$$

where P and M represent the electric and the magnetic dipole operators, respectively, and Im means the "imaginary part of." Analogous to the eq 3, it holds that $R(^2\Gamma) = b^2R(^4T_2)$; then

$$R(^2\Gamma) = b^2\text{Im}\langle^4T_2|P|^4A_2\rangle \cdot \langle^4A_2|M|^4T_2\rangle \tag{5}$$

These matrix elements of $R(^2\Gamma)$ can be obtained by using the Wigner and Clebsh–Gordan coefficients.[14,16] The rotational strengths of the zero-field splitting levels are summarized in Table II, where $R(^4A_1)$ and $R(^4E)$ are given by $\text{Im}\langle^4A_1|P|^4A_2\rangle \cdot \langle^4A_2|M|^4A_1\rangle$ and $2\text{Im}\langle^4E|P|^4A_2\rangle \cdot \langle^4A_2|M|^4E\rangle$, respectively.

Table II shows that the rotational strengths for the spin-forbidden transitions, $R(^2\Gamma)$, are represented by those for the first spin-allowed transitions to the ^4E and $^4A_1$ trigonal splitting components of the $^4T_{2g}$ state, $R(^4E)$ and $R(^4A_1)$. It is noticed that $R(^2E)$ ($=R(2\bar{A}) + R(\bar{E})$) and $R(^2T_1)$ ($=R(2\bar{A}) + R(\bar{E}_a) + R(\bar{E}_b)$) are proportional to the net rotational strength for the first spin-allowed transition, $R(^4E) + R(^4A_1)$. If the sum rule for the rotational strengths holds in the first spin-allowed transition,[17]

(14) S. Sugano and Y. Tanabe, *J. Phys. Soc. Jap.*, **13**, 880 (1958).
(15) E. U. Condon, *Rev. Mod. Phys.*, **9**, 423 (1937).
(16) S. Sugano, Y. Tanabe, and H. Kamimura, "Multiplets of Transition Metal Ions in Crystals," Academic Press, New York, N. Y., 1970.
(17) S. Sugano, *J. Chem. Phys.*, **33**, 1883 (1960).
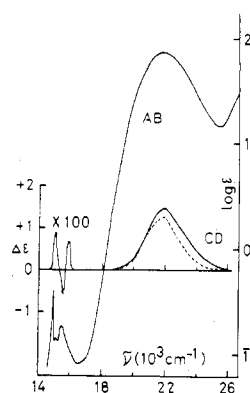
Figure 2. Absorption (AB) and CD curves of $(+)_{546}[\text{Cr(en)}_3]^{3+}$ in water (———) and in 0.4 F Na$_2$SeO$_3$ solution (- - - - -).

$R(^2E)$ and $R(^2T_1)$ vanish. It has been found, however, that the CD intensity of the $^4E \leftarrow {}^4A_2$ transition was stronger than that of the $^4A_1 \leftarrow {}^4A_2$ transition.[18] Thus, $R(^4E) + R(^4A_1)$ is different from zero and may be of same sign as $R(^4E)$. If the zero-field splitting of each ^2E and $^2T_1$ state is too small to be resolved by the room-temperature spectral measurements in solution, two CD bands due to the ^2E and $^2T_1 \leftarrow {}^4A_2$ transitions may be observed and should be of same sign as the major CD band in the first spin-allowed band region, owing to the separation between the ^2E and $^2T_1$ states which is large enough to be resolved spectroscopically. Since the zero-field splitting is caused by means of the combined interaction of the spin–orbit coupling and lower symmetry field, the energy interval of the $2\bar{A}$ and $\bar{E}$ components of the ^2E state is given by[14]

$$\lambda = E(2\bar{A}) - E(\bar{E}) = \frac{4K\zeta'}{E(^2E) - E(^2T_2)} \tag{6}$$

where $E(^2E)$ and $E(^2T_2)$ represent the energies of the $^2E \leftarrow {}^4A_2$ and $^2T_2 \leftarrow {}^4A_2$ transitions, respectively, the trigonal splitting parameter, K, equals $^2/_3 [E(^4E) - E(^4A_1)]$, and ζ' is the spin–orbit coupling constant; λ is found to be of the order of magnitude of 10 cm^{-1}.[2,12,13] Therefore, this splitting may be ignored in general. In particular cases, however, this must be taken into consideration. For the $^2T_1$ state, on the other hand, it has been revealed that the energy intervals of three zero-field splitting components depend largely upon the configurational interactions with the upper doublet states of the $(t_2)^2(e)$ configuration.[19] Thus, the assignment for the $^2T_1$ splitting components cannot be so explicitly determined as for the ^2E components.

$(+)_{546}$-**Tris(ethylenediamine) Complex.** The CD measurement of the $(+)_{546}$-tris(ethylenediamine)chromium(III) complex demonstrates that three sharp weak peaks, (+), (−), and (+), are observed in the region corresponding to the spin-forbidden transitions (Figure 2). The transition energy of the lowest frequency CD peak agrees well with those of the absorption and the phosphorescence spectra[4] (Table III). In addition, since the zero-field splitting of the ^2E state is found to be much smaller (18 cm^{-1}) than the CD half-bandwidth of about 200 cm^{-1},[20] the lowest frequency

(18) A. J. McCaffery and S. F. Mason, *Mol. Phys.*, **6**, 359 (1963); A. J. McCaffery, S. F. Mason, and B. J. Norman, *J. Chem. Soc.*, **2883** (1965).
(19) S. Sugano and M. Peter, *Phys. Rev.*, **122**, 381 (1961); R. M. Macfarlane, *J. Chem. Phys.*, **39**, 3118 (1963); R. M. Macfarlane, *ibid.*, **47**, 2066 (1967).
(20) I. B. Trabjerg and C. J. Ballhausen, *Mol. Phys.*, **20**, 811 (1971).

Table III. Absorption (AB) and CD Data for Chromium(III) Complexes in the d–d Transitions (Wave Numbers Are in 10^3 cm^{-1}; CD Intensities Asterisked Are Multiplied by 10^3)

AB (log ϵ_{max})	CD ($\Delta\epsilon_{ext}$)	Assignment	AB (log ϵ_{max})	CD ($\Delta\epsilon_{ext}$)	Assignment
(+)$_{546}$[Cr(en)$_3$](ClO$_4$)$_3$			(+)$_{546}$[Cr(phen)$_3$](ClO$_4$)$_3$		
14.9 ($\bar{1}$.64)	15.0 (+8.9*)	$\bar{E}$, 2 $\bar{A}$ (^2E)	13.7^a	13.8 (+12.8*)	$\bar{E}$, 2 $\bar{A}$ (^2E)
15.2 ($\bar{1}$.20)	15.5 (−5.7*)	$\bar{E}_b$ ($^2T_1$)		14.5 (−7.7*)	$\bar{E}_b$ ($^2T_1$)
15.5 ($\bar{1}$.31)	15.8 (+6.8*)	2 $\bar{A}$ ($^2T_1$)	23.4 sh	21.9 (+2.48)	^4E ($^4T_2$)
21.9 (1.88)	21.9 (+1.49)	^4E ($^4T_2$)	(+)$_{589}$[Cr(ox)(dip)$_2$]Cl·4H$_2$O		
(+)$_{546}$[Cr(tn)$_3$](ClO$_4$)$_3$			13.9 (0.25)	13.6 (+5.6*)	$\bar{E}$, 2 $\bar{A}$ (^2E)
15.0 ($\bar{1}$.32)	15.1 (+2.2*)	$\bar{E}$, 2 $\bar{A}$ (^2E)	14.7 (0.28)	14.0 (−1.7*) } $\bar{E}_b$ ($^2T_1$)	
15.3 ($\bar{1}$.23)	15.6 (−0.5*)	$\bar{E}_b$ ($^2T_1$)		14.3 (−3.0*)	
15.8 ($\bar{1}$.28)	15.9 (+1.1*)	2 $\bar{A}$ ($^2T_1$)		14.9 (+2.0*)	2 $\bar{A}$ ($^2T_1$)
21.6 (1.77)	20.9 (+0.34)	^4E ($^4T_2$)	20.3 (1.80)	17.8 (−0.06)	$^4A_1$ ($^4T_2$)
(+)$_{546}$K[Cr(ox)$_2$(en)]·2H$_2$O				20.6 (+1.40)	^4E ($^4T_2$)
14.5 (0.19)	14.5 (>+7.5*)	$\bar{E}$, 2 $\bar{A}$ (^2E)	(+)$_{589}$[Cr(ox)(phen)$_2$]ClO$_4$·2.5H$_2$O in 70% HClO$_4$		
14.9 (ca. 0.2)	14.9 (<−10.3*)	$\bar{E}_b$ ($^2T_1$)	13.6 (ca. $\bar{1}$.90)	13.8 (+4.6*)	$\bar{E}$, 2 $\bar{A}$ (^2E)
	15.3 (>+11.3*)	2 $\bar{A}$ ($^2T_1$)	14.7 (ca. $\bar{1}$.92)	14.8 (−6.2*)	$\bar{E}_b$ ($^2T_1$)
18.8 (1.96)	16.8 (<−0.05)	$^4A_1$ ($^4T_2$)	20.3 (1.80)	18.4 (−0.84)	$^4A_1$ ($^4T_2$)
	19.4 (>+2.00)	^4E ($^4T_2$)		21.2 (+1.50)	^4E ($^4T_2$)
(+)$_{546}$K[Cr(ox)$_2$(dip)]·3H$_2$O			(−)$_{589}$[Cr(ox)(dip)(phen)]ClO$_4$·2H$_2$O		
13.9 ($\bar{1}$.84)	13.8 (>+4.5*)	$\bar{E}$, 2 $\bar{A}$ (^2E)	13.7 (0.07)	13.6 (−5.2*)	$\bar{E}$, 2 $\bar{A}$ (^2E)
14.4 (ca. $\bar{1}$.80)	14.3 (<−5.4*) } $\bar{E}_b$ ($^2T_1$)		14.3 (0.12)	14.3 (+2.1*)	$\bar{E}_b$ ($^2T_1$)
	14.5 (<−6.6*)		20.0 (1.78)	20.5 (−1.76)	^4E ($^4T_2$)
14.7 (ca. 0.06)	14.8 (>+1.7*)	2 $\bar{A}$ ($^2T_1$)	(−)$_{589}$[Cr$_2$(OH)$_2$(dip)$_2$(phen)$_2$](NO$_3$)$_4$·7H$_2$O^c		
18.3 (1.87)	17.0 (<−0.12)	$^4A_1$ ($^4T_2$)	13.7 sh	13.7 (−76.6*)	+$\frac{1}{2}$ U$_+$, +$\frac{1}{2}$ U$_-$ (^2E)
	19.5 (>+2.22)	^4E ($^4T_2$)		14.1 (−92.0*)	−$\frac{1}{2}$ U$_+$, −$\frac{1}{2}$ U$_-$ (^2E)
(+)$_{546}$K[Cr(ox)$_2$(phen)]·4H$_2$O				15.5 (+8.3*)	$\bar{E}_b$ ($^2T_1$)
14.1 (0.42)	13.9 (>+32.0*)	$\bar{E}$, 2 $\bar{A}$ ($^2T_1$)	18.7 (1.98)	18.7 (−6.82)	^4E ($^4T_2$)
14.7 (ca. 0.5)	14.4 (<−3.0*)	$\bar{E}_b$ ($^2T_1$)	(−)$_{589}$[Cr(biguanide)$_3$]Cl$_3$		
	14.7 (>+27.0*)	2 $\bar{A}$ ($^2T_1$)	13.19^b	13.1 (−8.0*)	2 $\bar{A}$ (^2E)
18.5 (1.89)	16.4 (<−0.13)	$^4A_1$ ($^4T_2$)	14.3 (ca. $\bar{1}$.84)	14.3 (+4.0*)	$\bar{E}$ (^2E)
	19.0 (>+2.46)	^4E ($^4T_2$)	14.9 (ca. $\bar{1}$.82)		
(+)$_{546}$[Cr(ox)(en)$_2$]Cl			21.8 (2.00)	19.2 (−2.78)	$^4A_1$ ($^4T_2$)
14.6 ($\bar{1}$.90)	14.7 (+12.9*)	$\bar{E}$, 2 $\bar{A}$ (^2E)		21.7 (+4.16)	^4E ($^4T_2$)
15.2 ($\bar{1}$.78)	15.2 (−6.4*)	$\bar{E}_b$ ($^2T_1$)			
	15.5 (+11.4*)	2 $\bar{A}$ ($^2T_1$)			
20.3 (1.98)	20.8 (+1.97)	^4E ($^4T_2$)			

^{a} The wave numbers were obtained from the phosphorescence measurements of J. L. Laver and P. W. Smith, *Chem. Commun.*, 769 (1968). ^{b} The wave numbers were obtained from the phosphorescence measurements of N. A. P. Kane-Maguire and C. H. Langford, *Chem. Commun.*, 895 (1971). ^{c} The intensities are given per one complex ion, *i.e.*, per two chromium(III) ions.

CD band of positive sign in the spin-forbidden transition region is safely assigned to the ^2E components [$\bar{E}$, 2 $\bar{A}$]. Thus, as is theoretically anticipated in Table II, the CD band due to the $^2E \leftarrow {}^4A_2$ transition should be of same signs as the major CD band in the first spin-allowed $^4T_2 \leftarrow {}^4A_2$ transition. This case is the finding. The remaining two CD bands at the higher frequency side are ascribed to the $^2T_1 \leftarrow {}^4A_2$ transitions. That these CD bands are of opposite signs precludes assigning them to the [2 $\bar{A}$, $\bar{E}_b$] and $\bar{E}_a$ components of the $^2T_1$ state, for which the rotational strengths are proportional to the net rotational strength for the first spin-allowed transitions. The assignment to [$\bar{E}_a$, $\bar{E}_b$] and 2 $\bar{A}$ or to $\bar{E}_b$ and [2 $\bar{A}$, $\bar{E}_a$] accounts for the CD signs of the two observed bands. That is, the rotational strengths of the [$\bar{E}_a$, $\bar{E}_b$] and 2 $\bar{A}$ or of the $\bar{E}_b$ and [2 $\bar{A}$, $\bar{E}_a$] components are expected to be of opposite signs, because $R(^4A_1)$ contributes largely to R [$\bar{E}_a$, $\bar{E}_b$] and $R(\bar{E}_b)$ and because the rotational strength for the $^4E \leftarrow {}^4A_2$ transition, which contributes largely to $R(2\ \bar{A})$ and R [2 $\bar{A}$, $\bar{E}_a$], should have[17] a sign opposite to that of $R(^4A_1)$ (Table II). Judging from the fact that the CD intensities of the observed two bands due to the $^2T_1$ transitions are comparable to that of the lowest frequency CD band due to the ^2E transition and from the theoretical relationship that $R(\bar{E}_a)$ is $^3/_{32}$ times as small as $R(^2E)$ as shown in Table II, the $\bar{E}_a$ component may provide a minor contribution to the CD intensities of these bands, and the CD signs of these bands may depend upon

those of the rotational strengths for the 2 $\bar{A}$ and $\bar{E}_b$ components. Accordingly, the allocation of the $\bar{E}_a$ component cannot be determined by the CD measurement. Whether the positive CD band in the $^2T_1$ transition region is assigned to $\bar{E}_b$ or 2 $\bar{A}$ is responsible for the assignment of the major CD band in the first spin-allowed transitions to the ^4E or $^4A_1$ component. Since the intensity of the positive CD band in the first band region is diminished with the addition of sodium selenite to the solution (Figure 2) and since the Λ absolute configuration of (+)$_{546}$ isomer of this complex has been confirmed from the method of so-called "active racemates" by means of X-ray powder photographs,[21] the positive CD band is due to the ^4E component. In this case, therefore, the central negative and the highest frequency positive CD peaks in the spin-forbidden transition region may be assigned to the $\bar{E}_b$ and 2 $\bar{A}$ components, respectively.

Other Tris-Chelate Complexes. (a) (+)$_{546}$-Tris-(trimethylenediamine) Complex. As shown in Table III, for the (+)$_{546}$-tris(trimethylenediamine) complex (+)$_{546}$-[Cr(tn)$_3$]$^{3+}$ three sharp and weak CD peaks in the spin-forbidden band region and a positive CD band in the first

(21) P. Andersen, F. Galsbøl and S. E. Harnung, *Acta Chem. Scand.*, 23, 3027 (1969). The symbols Δ and Λ used in this paper agree with the designation of Andersen, *et al.*, and with "Nomenclature of Inorganic Chemistry; Definitive Rules 1970," Butterworths, London, 1971, p 75.

spin-allowed band region are observed, similar to the case of $(+)_{546}[\text{Cr(en)}_3]^{3+}$. Therefore, among three CD peaks, the lowest frequency positive one is assigned to $[2\bar{\text{A}}, \bar{\text{E}}(^2\text{E})]$. On the basis of the ion-pairing effect on the CD band in the first band region, a positive CD band may be assigned to the ^4E trigonal-splitting component of the $^4\text{T}_{2g}$ state,[9,22,23] and the absolute configuration of $(+)_{546}[\text{Cr(tn)}_3]^{3+}$ may be determined to be Λ. Accordingly, the central and the highest frequency CD peaks, $(-)$ and $(+)$, in the spin-forbidden band region may be assigned to the $\bar{\text{E}}_b$ and $2\bar{\text{A}}(^2\text{T}_1)$ components, respectively.

(b) **Complexes of Lower Symmetry.** Since the Kramers doublets are no longer split in any lower symmetry field, the correlation between the rotational strengths for the spin-forbidden and for the spin-allowed transitions will be applicable to the mixed complexes of lower symmetry.

The optically active mixed chromium(III) complexes containing three bidentate ligands show a CD pattern similar to that of the tris(ethylenediamine) complex in the spin-forbidden transition region; that is, three CD peaks are observed and the lowest and the highest frequency CD peaks are of opposite sign to the central one (Table III). The lowest frequency absorption or the highest frequency phosphorescence and the lowest frequency CD band of the complexes concerned coincide with each other in transition energy as in Table III. The sign of the lowest frequency CD peak in this region is found to be the same as that of the major CD band in the first spin-allowed band region. Therefore, this CD peak is due to the $^2\text{E}(\bar{\text{E}}, 2\bar{\text{A}})$ components. The absolute configuration determined on the basis of the CD dominance in the first spin-allowed band region is in accordance with that based on the other methods, *e.g.*, the observance exciton CD bands in the ligand band region of bis(2,2′-dipyridyl) and tris- or bis(1,10-phenanthroline) complexes[8,9] and the comparison between the CD spectra of the bis(oxalato) complexes and of the binuclear L-tartrato complexes with the $[\Delta$-$\Delta]$ configuration enforced by the stereospecificity.[24] Accordingly, since the major CD band in the first band region may be due to the ^4E trigonal parentage, the remaining higher frequency CD peaks in the spin-forbidden band region are assigned to the $\bar{\text{E}}_b$ and $2\bar{\text{A}}$ components of the $^2\text{T}_1$ state from the lower frequency side, respectively, according the parent trigonal notation as shown in Table III.

Two central negative CD peaks in the spin-forbidden transition region are observed for the 2,2′-dipyridyl complexes $(+)_{546}[\text{Cr(ox)}_2(\text{dip})]^-$ and $(+)_{589}[\text{Cr(ox)(dip)}_2]^+$. Such a splitting may be ascribed to the vibrational structure associated with the $\bar{\text{E}}_b(^2\text{T}_1) \leftarrow {}^4\text{A}_2$ electronic transition.

As seen in Figure 3, the μ-diol binuclear complex $(-)_{589}$-$[\text{Cr}_2(\text{OH})_2(\text{dip})_2(\text{phen})_2]^{4+}$ shows the splitting of the lower frequency CD bands due to the $^2\text{E} \leftarrow {}^4\text{A}_2$ transition similar to the case of $(-)_{589}[\text{Cr}_2(\text{OH})_2(\text{dip})_4]^{4+}$ and $(-)_{589}[\text{Cr}_2(\text{OH})_2$-$(\text{phen})_4]^{4+}$.[8] Mason suggested the spin-spin coupling

(22) P. G. Beddoe and S. F. Mason, *Inorg. Nucl. Chem. Lett.*, 4, 433 (1968); J. R. Gollogly and C. J. Hawkins, *Chem. Commun.*, 689 (1968).

(23) The ion-pairing effect on the CD band of the corresponding cobalt(III) complex, $(+)_{546}[\text{Co(tn)}_3]^{3+}$, was questioned: R. R. Judkins and D. J. Royer, *Inorg. Nucl. Chem. Lett.*, 6, 305 (1970). However, some doubts have been thrown on their proposal: C. J. Hawkins, "Absolute Configuration of Metal Complexes," Wiley-Interscience, New York, N. Y., 1970, pp 176, 211; P. G. Beddoe, M. J. Harding, S. F. Mason, and B. J. Peart, *Chem. Commun.*, 1283 (1971); K. R. Butler and M. R. Snow, *Inorg. Chem.*, 10, 1838 (1971).

(24) S. Kaizaki, J. Hidaka, and Y. Shimura, *Bull. Chem. Soc. Jap.*, 42, 988 (1969).

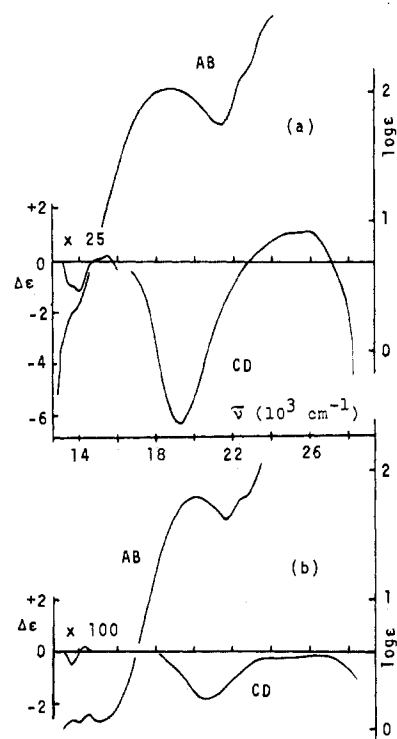**Figure 3.** Absorption (AB) and CD curves of $(-)_{589}[\text{Cr}_2(\text{OH})_2(\text{dip})_2$-$(\text{phen})_2]^{4+}$ (a) and $(-)_{589}[\text{Cr(ox)(dip)(phen)}]^+$ (b) in water.
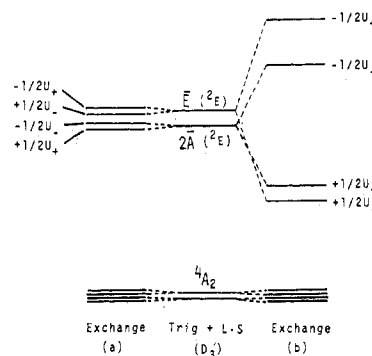

Figure 4. The splitting patterns of the ^2E state due to the exchange interaction in a binuclear complex. $\pm^1/_2\,\text{U}_-$ and $\pm^1/_2\,\text{U}_+$ refer to the wave functions of the ^2E state.

between the excited doublet states in these binuclear complexes. The exchange interaction causes the splitting of the two Kramers doublets, $2\bar{\text{A}}$ and $\bar{\text{E}}$, of the ^2E state as shown in Figure 4. If the splitting pattern follows (a) in Figure 4 and if the exchange splitting energy in the ground and the excited states is small enough to be neglected, the rotational strengths for the splitting components would correspond to $R(2\bar{\text{A}})$ and $R(\bar{\text{E}})$ and should have signs opposite each other. This case is not the finding. The splitting pattern (b), which is expected by the theoretical study of Sugano and Tanabe,[14] accounts for the two observed CD components of same signs. That is, assuming that two components of the upper $(-^1/_2\text{U}_-, -^1/_2\text{U}_+)$ or the lower $(+^1/_2\text{U}_-, +^1/_2\text{U}_+)$ pair locate closely each other, the rotational strengths for the upper and the lower pair, $[R(-^1/_2\text{U}_-) + R(-^1/_2\text{U}_+)]$ and $[R(+^1/_2\text{U}_-) + R(+^1/_2\text{U}_+)]$, are proportional to the net rotational strength for the first spin-allowed transitions, $R(^4\text{E}) + R(^4\text{A}_1)$, and should be of the same sign and also of the same sign as the major CD band in the first band region.
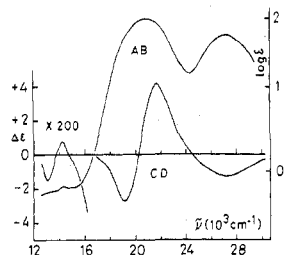
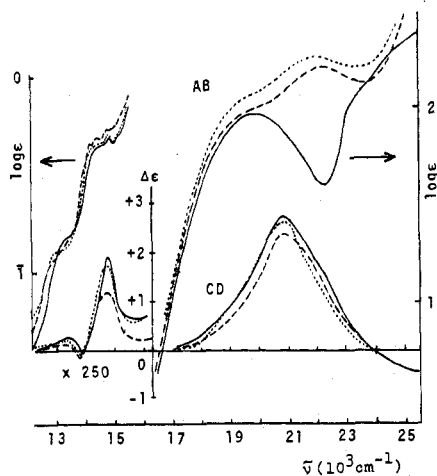**Figure 5.** Absorption (AB) and CD curves of $(-)_{589}[Cr(biguanide)_3]^{3+}$ in water.

Figure 6. Absorption (AB) and CD curves of $(+)_{546}[Cr(acac)(en)_2]^{2+}$ (———), $(+)_{546}[Cr(acaCl)(en)_2]^{2+}$ (· · · · ·), and $(+)_{546}[Cr(acaBr)$-$(en)_2]^{2+}$ (- - - - -) in water.

This is consistent with the observed CD behavior. Thus, the two CD components of the same sign may be assigned to $(+^1/_2 U_-, +^1/_2 U_+)$ and $(-^1/_2 U_-, -^1/_2 U_+)$ from the lower frequency side. The highest frequency negative CD band in the spin-forbidden band region is assigned to $\bar{E}_b(^2T_1)$.

$(-)_{589}$-**Tris(biguanide) Complex.** The $(-)_{589}$-biguanide complex shows two intense CD bands, $(+)$ at 22 kK and $(-)$ at 19 kK, in the first spin-allowed band region[25] (Figure 5). The absolute configuration of the $(-)_{589}$ isomer has been recently determined to be a Λ one by means of the X-ray analysis of the d-10-camphorsulfonate.[26] Thus, the positive major CD band may be assigned to the ^4E and the negative minor band to the $^4A_1$ trigonal splitting component of the $^4T_{2g}$ transition. In the region of the spin-forbidden transition, two weak and broad CD bands $(-)$ and $(+)$, were observed from the lower frequency side (Figure 5). Assuming that the lowest frequency CD component in the spin-forbidden transition is due to both the $2\bar{A}$ and $\bar{E}$ components of the ^2E state, this CD peak should be of positive sign, since the sign of $R(^2E)$ is the same as that of the net rotational strength for the first spin-allowed transition, $R(^4E) + R(^4A_1)$. However, the observed CD sign is negative. If the observed lowest frequency CD component is due to the $2\bar{A}$ or $\bar{E}$ zero-field splitting component of the ^2E state, the observation may be interpreted as follows. The energy ordering of the $2\bar{A}$ and $\bar{E}$ components (the interval is given by λ) depends upon the sign of the trigonal splitting parameter, K, which takes a positive or negative sign from one complex to another, as shown in eq 6, although
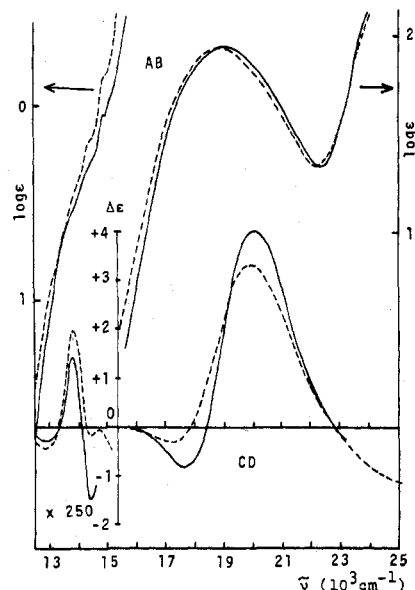
Figure 7. Absorption (AB) and CD curves of $(+)_{546}[Cr(acac)_2(en)]^+$ in water (———) and in methanol (- - - - -).

no strict proportionality has been found between the ^2E and $^4T_2$ splittings, λ and K, experimentally.[27] That is, the $2\bar{A}$ component is at the lowest frequency when K is positive, and *vice versa*. In the case of this complex, since K is assumed to be positive from the CD pattern in the first spin-allowed band region (Table III), the lowest frequency CD component is due to the $2\bar{A}$ and the highest frequency one is due to the $\bar{E}$ component. From Table II, the $2\bar{A}$ and $\bar{E}$ components are expected to have a negative and a positive sign, respectively, because $R(^4A_1)$ and $R(^4E)$ contribute largely to $R(2\bar{A})$ and $R(\bar{E})$, respectively. This is actually observed in the CD measurements of this complex. The zero-field splitting of the ^2E state of 1200 cm^{-1} is too large to be estimated from eq 6. When two neighboring CD components are broad and have opposite signs, the splitting interval observed is only apparent and much larger than the actual splitting interval as is seen in the case of the trigonal splitting of $(+)_{589}[Co(en)_3]^{3+}$ [28] or the exciton splitting of tris- and bis(α-diimine)metal complexes.[29]

The Acetylacetonato Complexes. (a) General Characteristics. The absorption and CD spectra of the acetylacetonato (acac) complexes $(+)_{546}[Cr(acac)(en)_2]^{2+}$ and $(+)_{546}[Cr(acac)_2(en)]^+$ and the corresponding 3-halogenacetylacetonato (acaX) complexes in the visible and near-infrared region are given in Figures 6–10, and their characteristics are summarized in Tables IV and V. The distinct absorption band with moderate intensity appearing in the visible region of mono- and bis(acetylacetonato) complexes is assigned to the first spin-allowed d–d transition. The shift of the position of the first band of tris-, bis-, and mono(acetylacetonato) complexes to the lower frequency side in this order is in accordance with the theoretical prediction.[30] The first absorption bands of $[Cr(acac)(en)_2]^{2+}$ and $[Cr(acac)_2(en)]^+$ are similar in position and in intensity to those of the corresponding

(25) K. Michelsen, *Acta Chem. Scand.*, 19, 1175 (1965).

(26) G. R. Brubaker and L. E. Webb, *J. Amer. Chem. Soc.*, 91, 7199 (1969).

(27) Y. Kawasaki and L. S. Forster, *J. Chem. Phys.*, 50, 1010 (1969).

(28) R. Dingle and C. J. Ballhausen, *Kgl. Dan. Vidensk. Selsk., Mat.-Fys. Medd.*, 35, No. 12 (1967).

(29) R. G. Bray, J. Ferguson, and C. J. Hawkins, *Aust. J. Chem.*, 22, 2091 (1969).

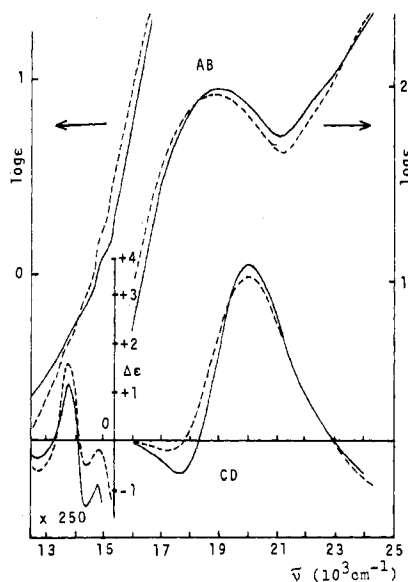(30) H. Yamatera, *Bull. Chem. Soc. Jap.*, 31, 95 (1958).

Figure 8. Absorption (AB) and CD curves of (+)$_{546}$[Cr(acac)(acaBr)-(en)]$^+$ in water (———) and in methanol (- - - - -).

Figure 10. Absorption (AB) and CD curves of (+)$_{546}$[Cr(acaCl)$_2$-(en)]$^+$ in water (———) and in methanol (- - - - -).

Table IV. Absorption (AB) and CD Data for Mono(acetylacetonato) Complexes in the d–d Transitions (Wave Numbers Are in 10^3 cm^{-1}; CD Intensities Asterisked Are Multiplied by 10^3)

AB (log ϵ_{max})	CD ($\Delta\epsilon_{ext}$)	Assignment
	(+)$_{546}$[Cr(acac)(en)$_2$]Cl$_2$·H$_2$O	
13.5 (*ca.* $\bar{1}$.15)	13.8 (+10.0*)	$\bar{E}$ (^{2}E)
14.8 (*ca.* $\bar{1}$.60)	14.2 (−1.30*)	2 $\bar{A}$ (^{2}E)
15.2 ($\bar{1}$.69)	15.2 (+77.0*)	$\bar{E}_a$, $\bar{E}_b$, 2 $\bar{A}$ (^{2}T$_1$)
20.2 (1.96)	21.1 (+2.75)	^{4}E (^{4}T$_2$)
	(+)$_{546}$[Cr(acaCl)(en)$_2$]Cl$_2$·1.5H$_2$O	
13.3 (*ca.* $\bar{1}$.10)	13.7 (+7.8*)	$\bar{E}$ (^{2}E)
14.6 (*ca.* $\bar{1}$.63)	14.2 (−3.2*)	2 $\bar{A}$ (^{2}E)
14.8 ($\bar{1}$.68)	15.1 (+69.0*)	$\bar{E}_a$, $\bar{E}_b$, 2 $\bar{A}$ (^{2}T$_1$)
15.2 ($\bar{1}$.71)		
20.0 (*ca.* 2.0)	21.1 (+2.62)	^{4}E (^{4}T$_2$)
22.3 (2.24)		
	(+)$_{546}$[Cr(acaBr)(en)$_2$]Cl$_2$·2.5H$_2$O	
13.2 (*ca.* $\bar{1}$.05)	13.7 (+5.4*)	$\bar{E}$ (^{2}E)
14.6 ($\bar{1}$.68)	14.2 (−5.6*)	2 $\bar{A}$ (^{2}E)
14.8 ($\bar{1}$.69)	15.2 (+48.0*)	$\bar{E}_a$, $\bar{E}_b$, 2 $\bar{A}$ (^{2}T$_1$)
15.2 ($\bar{1}$.73)		
20.0 (*ca.* 2.0)	21.2 (+2.38)	^{4}E (^{4}T$_2$)
22.5 (2.19)		

Figure 9. Absorption (AB) and CD curves of (+)$_{546}$[Cr(acaBr)$_2$(en)]$^+$ in water (———) and in methanol (- - - - -).

oxalato complexes [Cr(ox)(en)$_2$]$^+$ and [Cr(ox)$_2$(en)]$^-$, respectively, though the first bands of the 3-halogeno-substituted derivatives of the mono(acetylacetonato) complex are observed as shoulders on the low-frequency side of the new absorption bands appearing at about 22 kK (Figure 6). The similarity of the first absorption band between the acetylacetonato and the oxalato complexes corresponds to the fact that the ligand field strength parameter, Δ, of the acetylacetonate is close but somewhat larger than that of the oxalato ligand.[31]

The CD curves of these complexes in the first absorption band region are also of the similar shape to the corresponding oxalato complexes, although the CD intensities of the acetylacetonato complexes are stronger than those of the oxalato complexes (Tables III-V). The CD bands of the
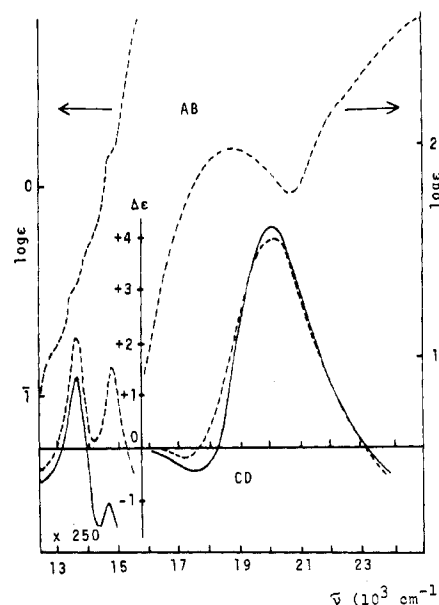
mono(3-halogenoacetylacetonato) complexes in the first band region are undisturbed by the newly appearing absorption band and similar to that of the corresponding acetylacetonato complex. Therefore, the new band near 22 kK is suggested to be due to an optically active or magnetic dipole forbidden transition.

Contrary to the region of the first spin-allowed d–d absorption band, the spin-forbidden absorption bands of the acetylacetonato complexes are distinguished from those of the oxalato complexes. As is shown in Tables III-V, the spin-forbidden bands of the acetylacetonato complexes are shifted to lower frequencies than those of the oxalato complexes and also to higher frequencies than those of the 3-halogenoacetylacetonato complexes as in the case of tris(acetylacetonato) and tris(3-halogenoacetylacetonato) complexes,[32] indicating the nephelauxetic effect.[33] The broad-

(31) Y. Shimura and R. Tsuchida, *Bull. Chem. Soc. Jap.*, **29**, 311 (1956).

(32) K. DeArmond and L. S. Forster, *Spectrochim. Acta*, **19**, 1403 (1963).

(33) C. K. Jorgensen, "Absorption Spectra and Chemical Bonding," Pergamon Press, Oxford, 1962, p 134.

Table V. Absorption (AB) and CD Data for Bis(acetylacetonato) Complexes in the d–d Transitions (Wave Numbers Are in 10^3 cm^{-1}; CD Intensities Asterisked Are Multiplied by 10^3)

In water		In methanol		
AB (log ϵ_{max})	CD ($\Delta\epsilon_{ext}$)	AB (log ϵ_{max})	CD ($\Delta\epsilon_{ext}$)	Assignment
(+)$_{546}$[Cr(acac)$_2$(en)]Cl·1.5H$_2$O				
13.3 sh	12.9 (−11.9*)		12.9 (−18.6*)	$2\,\bar{A}$ (^{2}E)
13.7 sh	13.9 (+56.0*)	14.3 sh	13.9 (+78.5*)	$\bar{E}$ (^{2}E)
15.0 ($\bar{1}$.95)	14.5 (−22.4*)	15.0 sh	14.5 (−7.40*)	$\bar{E}_b$ (^{2}T$_1$)
19.0 (1.95)	17.7 (−0.84)	18.9 (1.94)	17.3 (−0.29)	^{4}A$_1$ (^{4}T$_2$)
	20.1 (+4.00)		20.0 (+3.30)	^{4}E (^{4}T$_2$)
(+)$_{546}$[Cr(acac)(acaBr)(en)]Cl·H$_2$O				
	12.7 (−13.9*)		12.7 (−21.7*)	$2\,\bar{A}$ (^{2}E)
	13.8 (+48.3*)	14.0 sh	13.8 (+63.0*)	$\bar{E}$ (^{2}E)
15.0 sh	14.4 (−54.3*)	15.0 sh	14.4 (−21.7*)	$\bar{E}_b$ (^{2}T$_1$)
19.0 (1.95)	17.7 (−0.84)	18.7 (1.96)	17.2 (−0.22)	^{4}A$_1$ (^{4}T$_2$)
	20.1 (+3.59)		20.0 (+3.35)	^{4}E (^{4}T$_2$)
(+)$_{546}$[Cr(acaBr)$_2$(en)]Cl$_{0.5}$Br$_{0.5}$				
			12.7 (−12.4*)	$2\,\bar{A}$ (^{2}E)
			13.7 (+86.4*)	$\bar{E}$ (^{2}E)
		15.0 sh	14.9 (+52.9*)	$2\,A$ (^{2}T$_1$)
19.0 (2.02)	17.3 (−0.88)	18.7 (2.00)	17.7 (−0.13)	^{4}A$_1$ (^{4}T$_2$)
	20.2 (+4.40)		20.2 (+4.13)	^{4}E (^{4}T$_2$)
(+)$_{546}$[Cr(acaCl)$_2$(en)]Cl·H$_2$O				
	12.6 (−25.2*)		12.6 (−15.0*)	$2\,\bar{A}$ (^{2}E)
	13.7 (+54.5*)	13.0 sh	13.7 (+84.5*)	$\bar{E}$ (^{2}E)
	14.5 (−60.3*)	13.6 sh		$\bar{E}_b$ (^{2}T$_1$)
		14.9 sh	14.9 (+61.5*)	$2\,A$ (^{2}T$_1$)
18.9 (2.00)	17.7 (−0.86)	18.7 (1.98)	17.3 (−0.17)	^{4}A$_1$ (^{4}T$_2$)
	20.2 (+4.21)		20.0 (+3.94)	^{4}E (^{4}T$_2$)

ness of the bandwidth, the large energy intervals, and the irregular intensity ratios of the CD bands in the spin-forbidden band region are highly characteristic of the acetylacetonato complexes.

(b) The Mono(acetylacetonato) Complexes. The (+)$_{546}$ isomers of these complexes exhibit a positive intense CD band in the first spin-allowed band region. Thus, these complexes may have a Λ absolute configuration. The absorption measurements of the mono(acetylacetonato) complexes in the near-infrared region demonstrate that a weak shoulder and a relatively intense plateau with some inflections are observed from the lower frequency side (Figure 6). In the corresponding region, three CD peaks, (+), (−), and (+), are observed (Figure 6); two of them at the lower frequency are of weak intensity, and the highest frequency positive peak is of relatively strong intensity and broad. That is, the strong but broad CD band belongs to the highest frequency relatively intense plateau in absorption spectrum and the other less intense CD bands may correspond to the lower frequency weak shoulder of the spin-forbidden absorption bands. The interval between the shoulder and the plateau of the spin-forbidden absorption bands is about 1500 cm^{-1}, and the spacing of about 500 cm^{-1} between the positive lowest frequency and the negative central CD peak is much smaller than that between the central and the highest frequency CD peak (1000 cm^{-1}). Thus, it is likely that the central negative CD peak belongs to the lower frequency shoulder rather than to the higher frequency plateau. In general, it is found that the energy interval between the ^{2}E component and one of the ^{2}T$_1$ zero-field splitting components, $\bar{E}_b$ or $2\,\bar{A}$, is larger than that between the ^{2}T$_1$ components, $\bar{E}_b$ and $2\,\bar{A}$ (Table III). Accordingly, it seems questionable that the lowest frequency CD peak is due to the combined $2\,\bar{A}$ and $\bar{E}$ components of the ^{2}E ← ^{4}A$_2$ transition and the remaining bands are due to the ^{2}T$_1$ splitting components. The lowest frequency positive and the central negative CD

peaks of mono(acetylacetonato) complexes in the spin-forbidden band region are reasonably assigned to the $\bar{E}$ and $2\,\bar{A}$ components of the ^{2}E state, respectively, and the remaining positive intense CD band at the highest frequency side to the overall $\bar{E}_a$, $\bar{E}_b$, and $2\,\bar{A}$ components of the ^{2}T$_1$ state. The observed CD signs are consistent with those derived from the theoretical prediction. From Table II, the overall rotational strength for the ^{2}T$_1$ transitions is proportional to the net rotational strength for the first spin-allowed transition, $R(^4\text{E}) + R(^4\text{A}_1)$, and the signs of the rotational strengths for the $2\,\bar{A}$ and $\bar{E}$ components of the ^{2}E transitions depend upon those for the ^{4}A$_1$ and ^{4}E components of the ^{4}T$_{2g}$ transition, respectively. Therefore, in the case of (+)$_{546}$[Cr(acac)(en)$_2$]$^{2+}$, since the major CD band in the first spin-allowed band region is considered to be of dominant ^{4}E trigonal parentage, the highest frequency CD band should be of same sign as that of the major CD band in the first spin-allowed band region, and the lowest frequency and the central CD bands should be inverse in sign, positive and negative, respectively. This case is the finding.

The observed inflections on the top of the absorption plateau near 15 kK with the interval of about 200 and 400 cm^{-1} are probably due to the vibrational structures associated with the electronic transition to the ^{2}T$_1$ state.

(c) The Bis(acetylacetonato) Complexes. The CD measurements in the visible region of the (+)$_{546}$-bis-(acetylacetonato) complexes show two bands, a minor negative and a major positive one from the lower frequency side (Figure 7). Now, assuming that the bis(acetylacetonato) complexes belong to pseudo-D_3 symmetry, the positive major and the negative minor CD band in the first band region may be assigned to the ^{4}E and ^{4}A$_1$ trigonal parentage, respectively. And these complexes may take a Λ absolute configuration. This assignment of the absolute configuration coincides with that derived from the argument concerning the CD spectra in the ultraviolet region in the previous paper[1] as well as that from the X-ray determination[34] of the

analogous β-diketonato complex $\Lambda(+)_{589}$-*mer*-tris((+)-3-acetylcamphorato)chromium(III), showing a dominant positive CD component in the first absorption band region and a similar CD pattern in the ultraviolet region.[35]

The CD spectra of $(+)_{546}$-bis(acetylacetonato) complex in the spin-forbidden band region show three peaks, $(-)$, $(+)$, and $(-)$, in water (Figure 7). It has been demonstrated that the highest frequency negative CD component becomes weaker in methanol in the case of $(+)_{546}[Cr(acac)_2(en)]^+$ and $(+)_{546}[Cr(acac)(acaBr)(en)]^+$ (Figures 5 and 6 and Table V). Finally, in the case of $(+)_{546}[Cr(acaCl)_2(en)]^+$ and $(+)_{546}$-$[Cr(acaBr)_2(en)]^+$, the highest frequency negative CD band disappeared and a new positive intense band appeared at the higher frequency side in methanol (Figures 9 and 10 and Table V). Therefore, it is evident that there may exist four CD components, $(-)$, $(+)$, $(-)$, and $(+)$, in the spin-forbidden band region from the lower frequency side, although the reason for the change of intensity is uncertain. Since the sign of the lowest frequency CD peak in the spin-forbidden band region is opposite to that of the major CD band in the first spin-allowed absorption band region, as in the case of the $(-)_{589}$-tris(biguanide) complex, this CD peak seems to correspond to one of the zero-field splitting components of the ^2E state. Namely, since the trigonal splitting parameter, K, for these bis(acetylacetonato) complexes is positive, the lowest frequency negative CD peak may be assigned to the $2\bar{A}(^2E)$ and the positive next-to-lowest frequency intense CD peak may be assigned to the $\bar{E}(^2E)$ component. Since $R(^4A_1)$ is negative and $R(^4E)$ is positive, the signs for $R(2\bar{A})$ and for $R(\bar{E})$ are consistent with the observed CD signs, $(-)$ and $(+)$. The remaining CD peaks, of which the negative one becomes weaker and disappears in methanol and of which the positive one is not observable in water but newly appears in methanol, may be assigned to the $\bar{E}_b$ and $2\bar{A}$ of the $^2T_1$ splitting components, respectively. On the other hand, Armendarez and Forster[36] investigated the polarized

crystal absorption spectra of tris(acetylacetonato)chromium-(III) complex and of its 3-halogeno derivatives at low temperature in the spin-forbidden band region and observed many vibrational structures in the $^2E \leftarrow {}^4A_2$ and $^2T_1 \leftarrow {}^4A_2$ transitions. And they also measured the emission spectrum of tris(acetylacetonato) complex and found a poor mirror image between the absorption and emission spectra, especially in the range far distant from the 0–0 transition to the ^2E state. Thus, the observed relatively intense but broad absorption band near 14,400 cm^{-1} with the spacing of about 1600 cm^{-1} from the 0–0 transition at 12,882 cm^{-1} was assigned to the $^2T_1 \leftarrow {}^4A_2$ transitions. This spacing of about 1600 cm^{-1} from the $^2E \leftarrow {}^4A_2$ transitions agrees with the spacing of 1000–2000 cm^{-1} obtained from the CD measurements of the $(+)_{546}$ isomers of bis- and mono-(acetylacetonato) complexes. It is noticed that the energy interval of the ^2E and $^2T_1$ states for the acetylacetonato complexes is a few times as large as that for the oxalato and ethylenediamine complexes. The large zero-field splitting of the ^2E state for the acetylacetonato complexes (about 800 cm^{-1}) cannot be interpreted from a crystal field viewpoint by using eq 6. Such a large splitting of the ^2E and $^2T_1$ states seems to be ascribed to the delocalization of the π electrons of the ligand to the t_2 shell of the metal ion or to the strong configurational interactions between the ^2E or $^2T_1$ state and the ligand states of the same symmetry in the coordinated acetylacetonate.

(34) W. D. Horrocks, Jr., D. L. Johnston, and D. MacInnes, *J. Amer. Chem. Soc.*, **92**, 7620 (1970).

(35) R. M. King and G. W. Everett, Jr., *Inorg. Chem.*, **10**, 1237 (1971).

(36) P. X. Armendarez and L. S. Forster, *J. Chem. Phys.*, **40**, 273 (1964).